Design of a Dual-Polarized Omnidirectional Dielectric Resonator Antenna for Capsule Endoscopy System

JIANJUN LAI[1], JI WANG[2], KEJIA ZHAO[3], HAO JIANG[1], LITING CHEN[1], ZHIBING WU[1], AND JIPING LIU[4]

[1]Department of Oncology, Zhejiang Hospital, Hangzhou 310013, China
[2]Department of Medical Engineering, Zhejiang Hospital, Hangzhou 310013, China
[3]Department of Gastroenterology, Zhejiang Hospital, Hangzhou 310013, China
[4]Department of Radiation Physics, Cancer Hospital of the University of Chinese Academy of Sciences (Zhejiang Cancer Hospital), Institute of Basic Medicine and Cancer(IBMC), Chinese Academy of Sciences, Hangzhou 310022, China

Corresponding authors: Jiping Liu (liujp_2627@163.com) and Zhibing Wu (wu_zhibing@163.com)

ABSTRACT In this paper, a new dual-polarized (DP) omnidirectional hemisphere dielectric resonator antenna (DRA) for wireless capsule endoscope system (WCE) is proposed. The antenna was excited in its omnidirectional $TM_{01\delta}$ and $TE_{01\delta}$ modes to radiate DP wave by a feeding probe and arc microstrip line, respectively. Omnidirectional DP wave can be obtained when the $TM_{01\delta}$ and $TE_{01\delta}$ mode are equal in amplitude and phase. The $TM_{01\delta}$ mode that is equivalent to electric dipole can be obtained by probe feeding. The $TE_{01\delta}$ mode is excited by four arc microstrip lines feeding. They provide a pair of equivalent magnetic dipoles that are orthogonal to $TM_{01\delta}$ mode. The DP omnidirectional DRA be fabricated without the need of feed network than circularly polarized. The WCE and the human body equivalent tissue model are adopted in simulation. Water is equivalent to gastric juice during measurement. Communication links between the proposed capsule antenna and the external receiving antenna are measured to demonstrate the advantages the DP brings when capsule antenna is placed in different orientations. The capsule endoscope system with different antennas is placed in water to measure receiving power. The measurement shows that the fabricated antenna exhibits a wide impedance bandwidth for S11 < -10 dB (2.4–2.48 GHz). The radiation efficiency of the antenna is between 15-18%, and the peak gain is between -13.5 and -15dBi.

INDEX TERMS Dielectric resonator antenna, dual-polarized, omnidirectional, wireless capsule endoscope system.

I. INTRODUCTION

Wireless capsule endoscope system (WCE) has the technical characteristics of whole digestive tract examination, painless and non-invasive [1]. It can obtain the image information of gastrointestinal tract and realize the clinician's direct observation on the image of gastrointestinal lesions, so as to realize the diagnosis of gastrointestinal diseases [2], [3].

Among the numerous implanted medical systems, WCE system is a comprehensive integrating communication system including optoelectronic engineering, biomedicine and image processing. The antenna used for image data trans-

The associate editor coordinating the review of this manuscript and approving it for publication was Mohammed Bait-Suwailam.

mission is an important part for the wireless communication system [4]. When the WCE system is operating in the digestive tract, the sensor is responsible for collecting the internal information of the digestive tract [5]–[7]. The chip modulates these data signals and transmits them to the antenna, which sends the modulated signals to the external receiving device in the form of electromagnetic waves. The medical diagnosis needs to rely on a large number of high-resolution images, which requires the communication system to have high data transmission rate and broad bandwidth. The traditional antenna is no longer satisfied with the requirements of WCE system due to its large size, narrow bandwidth and complex structure. The antenna used for WCE is developing towards miniaturization, multi-function, broadband and

easy conformation. Because the antenna performance directly affects the data transmission quality of WCE system, it is of great significance and broad market prospect to research on WCE antenna [8], [9].

Given Imaging company is devoted to the development and experiment of capsule endoscope, and the company has made great achievements especially in the field of clinical application. In 2000, the company launched the world's first capsulated wireless endoscope, the M2A [10]. The WCE system antenna belongs to the category of implantable antenna. In the process of medical examination of patients, the antenna will keep moving inside the human body due to the influence of gravity and gastrointestinal peristalsis. This situation will make it difficult to determine the specific position and direction of the antenna, which requires the antenna to have good omni-directional radiation characteristics. When the antenna is miniaturized as much as possible, it is should also be considered how to keep the omni-directional radiation characteristics of the antenna.

The implantable antenna inside the body will rotate and move with the influence of gravity and gastrointestinal peristalsis. So the polarization direction of the antenna cannot be determined. If the internal antenna is linearly polarized, the angle between the implantable antenna and the external antenna will change. The situation will lead to the polarization mismatch and affect the communication quality. The body structure is complex, and it has features with high dielectric constant, non-uniform, high loss. The influence of antenna size, bandwidth, radiation efficiency and radiation to human body on the system should be considered. It is the difficult and hot spot of research to design high-performance implanted miniaturized antenna. In 2017, Professor Yong-Xin Guo's team from the National University of Singapore designed a small implantable circular-polarized antenna working in the ISM frequency band (2.4-2.48ghz), but the antenna did not achieve omnidirectional radiation characteristics [11]. In 2017, Hyoungsuk Yoo's team at Ulsan University in South Korea designed a wideband circular-polarized antenna for high-speed data transmission WCE system. The antenna is bent into a cylindrical shape so that it is conformal with capsule (11 mm × 26 mm). The size of the antenna is reduced by attaching curved slots of different lengths [12]. But electronic components, such as CMOS cameras, batteries and LED lights have serious effects on the radiation performance of the antenna [13]–[18].

Dielectric resonator antenna, which is made of material with high dielectric constant, is a kind of miniaturized antenna which is different from traditional antenna in radiation principle [19]–[22]. Because the material loss of dielectric resonator is usually very small, and there is no surface wave loss, the whole surface will produce electromagnetic wave radiation except the ground part, so the radiation efficiency of dielectric resonator antenna is generally very high [23]–[25].

In order to solve the problem of polarization mismatch, circular polarization antennas are mostly proposed. As is well
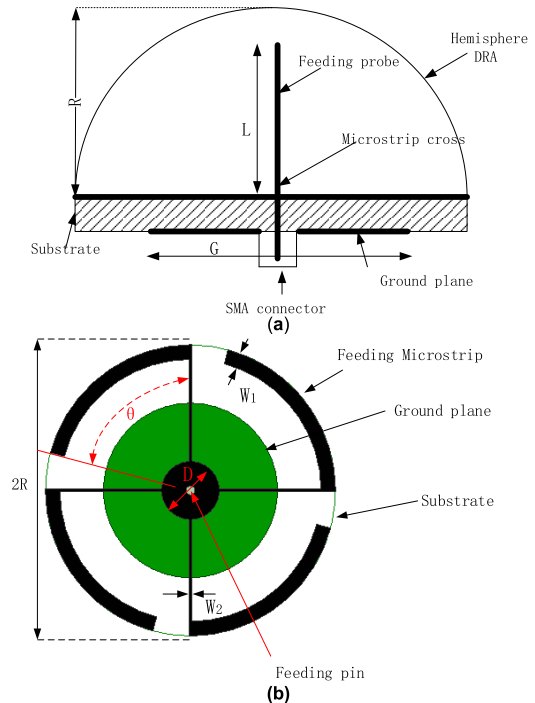

FIGURE 1. Geometry of the proposed antenna: (a) Top view; (b) Top view.

known, human body is a inhomogeneous object with electromagnetic (EM) material characteristics. However, the axial ratio of implantable circular polarized antenna is extremely unstable inside the human body because of the diversity and complexity of tissues. In this paper, the dual polarization omnidirectional DRA is proposed as the WCE transmitting antenna, which has the characteristics of miniaturization and stability. The problem of polarization mismatch can be solved, and the axial ratio can be ignored. The shape of the antenna is hemispherical, which is easy to be conformal with the end of the capsule. The antenna structure is simple and easy to process.

II. ANTENNA STRUCTURE DESIGN

Fig. 1 shows the configuration of the dual polarization omnidirectional hemispherical DRA that is fed by a planar arc-shaped microstrip and probe. The DRA has a dielectric constant of $\varepsilon_r = 22$, loss tangent of 0.002. The material is a mixture of ceramic and low-loss dielectric material. And the relative dielectric constant and loss tangent are provided by the processor after testing. A method of designing an omnidirectional dual polarization antenna is seen as an electric dipole and a magnetic dipole. This approach is adopted in designing an omnidirectional dual polarization DRA, where the electric and magnetic dipoles are realized by using the $TM_{01\delta}$ and $TE_{01\delta}$ mode of the DR, respectively. The height of the DRA was R = 5 mm. Fig. 1 (b) displays the feeding microstrip, which is printed on a circular substrate with a thickness of 0.5 mm, radius of R = 5 mm, and dielectric constant of $\varepsilon = 4.4$. The microstrip cross has a small circular

TABLE 1. Optimal value of structural parameters.

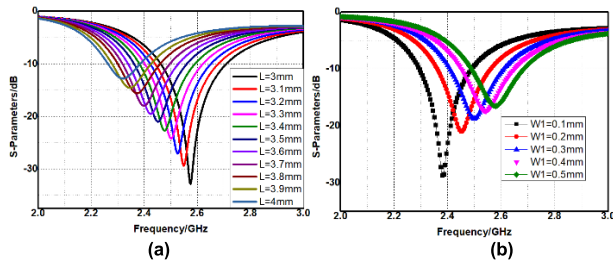| Parameters	Values	Parameters	Values
R	5mm	W1	0.4mm
G	3mm	W2	0.1mm
L	3.5mm	θ	70deg
D	1mm		

FIGURE 2. Reflection coefficient of the antenna for different liquid chemicals. (a) S11 with the feeding probe of different length L; (b) S11 with microstrip lines of different widths W1.

patch at the center and a diameter of D. The four feeding arc microstrip lines are connected by a microstrip line of width W2 with the center patch, respectively.

To feed the DRA, a probe is used in Fig. 1 (a). The proposed DRA resonates at 2.45 GHz with 10 dB bandwidth of 200 MHz (2.36–2.56 GHz, simulation result) covering most of the application ISM band. The compact structure of the antenna makes it a suitable choice for WCE applications. The final dimension of the dual polarization DRA was optimized with High Frequency Structure Simulator (HFSS) and the values are given in Table 1.

III. THE SIMULATION ANALYSIS
A. PARAMETERS ANALYSIS
The simulations using HFSS software for the parametric study were carried out. The influence of the length of the feed probe L and the width of the arc feed microstrip line W1 on the reflection coefficient of the dielectric resonant antenna is discussed. The influence of parameter L on the antenna performance is shown in the Fig. 2 (a). It can be seen from the figure that the operating frequency of the antenna moves to the low-frequency band with the increase of L. As shown in the Fig. 2 (b), the operating frequency shifts to the low-frequency band with the increase of W1. Considering the impedance of each parameter to the antenna performance and the shadow of radiation performance, the antenna finally chooses L as 3.5mm and W1 = 0.3mm as the optimal values. The impedance characteristic deteriorates to different arc microstrip line degrees θ. This parameter is not shown in the diagram. All these parameters are simulated with gastric juice and human tissue model without capsule structure.

The proposed antenna is a dual-polarization antenna. The radiation characteristics of the antenna are shown here, when fed with single-polarization. As shown in the Fig. 3 (a), the
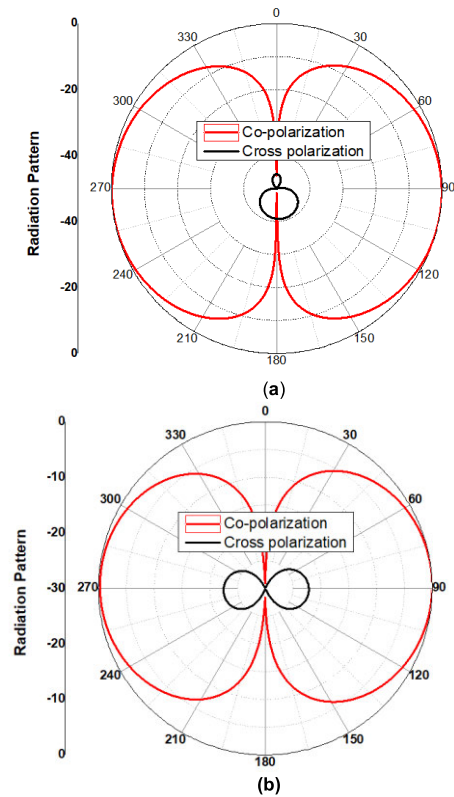

FIGURE 3. Radiation pattern with single polarization. (a) The co-polarization and cross polarization radiation patterns only with the probe feeding; (b) The co-polarization and cross polarization radiation patterns only with the microstrip feeding.

radiation characteristics of the dielectric resonant antenna are displayed with only feeding probe. The normalized radiation characteristics of the main polarization and cross-polarization of plane E are shown here. The feeding input impedance of the antenna was 100 Ω by this time. When the antenna is fed only by arc microstrip lines, the four arc microstrip lines form a current ring and the dielectric resonant antenna radiates omni-directional horizontal polarized electromagnetic waves. When the antenna is fed separately, the feeding port adopts 100 Ω as the input impedance. In this way, the final antenna input impedance is 50 Ω and the horizontal wave and vertical polarization wave have equal amplitude distribution.

B. ELECTRIC FIELD ANALSIS AND RADIATION PATTERN
The Fig. 4 shows the electric field distribution diagram of the antenna in different modes. When only the probe fed, dielectric resonance operates in $TM_{01\delta}$ mode, as shown in Figure 4 (a). At this time, the electric field inside the probe is in reverse with the electric field inside the dielectric resonance. When only the arc microstrip line fed, the antenna works in $TE_{01\delta}$ mode. The electric field distribution diagram of dielectric resonant antenna is shown in Figure 4 (b), and the electric field presents a circular characteristic at this time.

Normalized radiation pattern of dielectric resonance antenna with co-polarization and cross polarization was
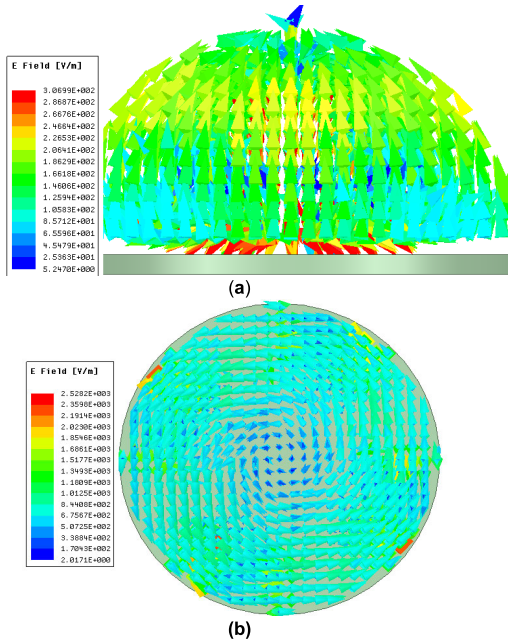
(a)

(b)

FIGURE 4. Simulated near fields of DP omnidirectional DRA using HFSS. (a) E-field in elevation (yz) plane at x = 0, when only the probe fed, (b) E-field in azimuthal (xy) plane at z = 0, when only the arc microstrip line fed.
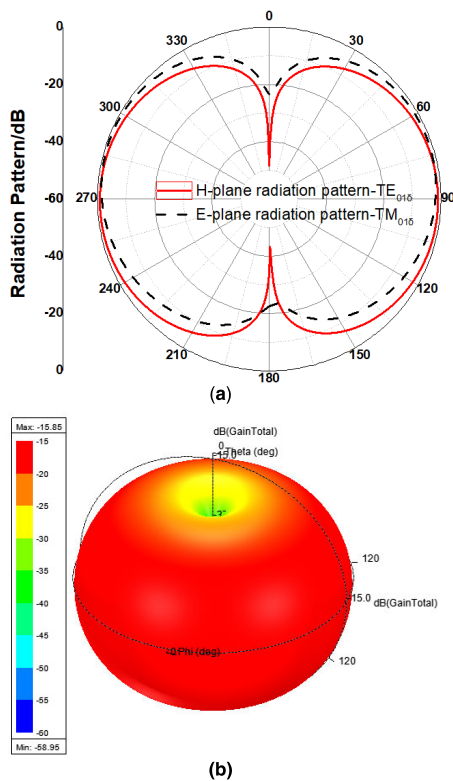

(a)

(b)

FIGURE 5. Radiation pattern of dielectric resonance antenna (a) 2D radiation pattern of co-polarization and cross polarization was shown; (b) 3Dgain radiation pattern.

shown in the Fig. 5 (a). The co-polarization is E-plane radiation pattern of vertically polarized electromagnetic wave and the cross polarization is H-plane radiation pattern of
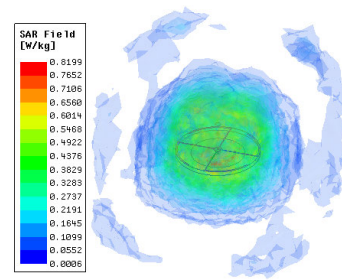

FIGURE 6. Distribution of the surface SAR.

horizontal polarized electromagnetic wave. The antenna has the characteristics of radiating dual-polarization electromagnetic waves. Figure (b) is the antenna three dimensions (3D) gain radiation pattern. When electromagnetic wave penetrates human tissue, it will bring about scattering and loss. So antenna gain is only −15dBi.

C. SAR AND COMPATIBILITY ANALYSIS

Specific Absorption Rate (SAR) refers to radio frequency energy absorbed by the human body. In the process of data and energy transmission between wireless implanted devices and external devices, the transmission of electromagnetic wave in human body will be absorbed by human body. The electromagnetic radiation absorbed by human body will lead to the increase of body temperature. The temperature rise of tissue around the implanted device should not exceed 1-2 °C. For the safety of human body, the radiation value to human body needs to be regulated. Therefore, all implantable devices must comply with the standard set by the IEEE for SAR. There are currently two IEEE (Institute of Electrical and Electronics Engineers) standards for reference [26]: (1) the IEEE c95.1-1999 standard limits the SAR value no more than 1.6 W/kg of 1g /m3 of human tissue for an input power of 2mW. (2) THE IEEE C95.1-2005 standard limits the SAR value no more than 2 W/kg of 1g /m3 of human tissue for an input power of 2mW. Peak SAR can be defined as:

$$\text{SAR} = \frac{1}{2}\frac{\sigma_e \, |E(r_0)|^2}{\rho(r_0)} \quad (1)$$

In formula (1), σ_e (S/ M) and ρ (kg/m3) represent the conductivity and mass density of the medium, respectively. Moreover, $1/2\sigma_e \, |E(r_0)|^2$ is the average energy density absorbed by the body in the point of r_0 place.

In this study, we use HFSS simulation software combined with a simple human tissue model to calculate the SAR value of human body under a specific input power. In figure6, the peak SAR value is 0.8199W/kg at 2.45 GHz under condition of 2mW input power.

Generally, electronic interference (EMI) refers to any electromagnetic disturbance that can cause the performance degradation of equipment signal transmission system; and electromagnetic disturbance is an electromagnetic phenomenon, which can reduce the performance of equipment system, and even endanger human health. For example,

the mobile phone carried by human beings will emit electromagnetic radiation. When the mobile phone is close to the electronic medical equipment, it will reduce the performance and accuracy of the equipment. There are three essential factors for electromagnetic interference to cause substantial damage.

(1) Interference source is the main body of interference, including electronic components, equipment and natural phenomena;

(2) Interference channel, also known as coupling channel, is the way for interference source to transmit disturbance energy to interference object. Generally, there are three kinds of coupling: direct coupling, inductive coupling and radiation coupling;

(3) Interference object, that is sensitive electronic components or equipment system interfered by interference source.

Electrostatic discharge (ESD): the contact discharge of ±4KV. Due to the non-metallic shell with biological compatibility of the capsule, the static electricity fails to produce a functional breakdown of the system.

To interference: 150 KHz - 80 MHz (80% amplitude modulation, 1 KHz frequency modulation) of the radio frequency interference sources in the form of electromagnetic wave produced interference in the equipment connecting cable, which generates current on the equipment. The data between capsule endoscope and receiver is transmitted wirelessly, and the conducted interference is mainly caused by the USB cable between the receiver and PC. By adding anti-interference magnetic ring on USB data line, the interference is reduced. And when the power circuit is designed, corresponding EMC analysis was considered; and by increasing the overvoltage, overcurrent and overheating protection circuit to weaken the conduction interference.

Radiation interference: Interference source (80 MHz-2.5GHz) with frequency modulation of 1KHz and amplitude modulation of 80%, field strength 3V/m generates induction current to sensitive parts (such as antenna) in the form of radiation electromagnetic waves, and then enters the equipment, causing interference to the equipment. The experimental results did not affect the function of the capsule endoscope. The capsule endoscope mainly radiated electromagnetic waves outward and only received startup and wake-up signals under certain signals.

D. WCE SYSTEM ANALYSIS

The overall structure of the WCE system is shown in the figure 7 (a), which includes the camera sensor, the data processing chip, the battery, the magnetic core used to control the orientation, the RF transmitter and the antenna. The overall size of capsule endoscope is 20 × 11 cm. Capsule endoscope shell is made of a special sealed biocompatible material, which can resist strong gastric acid and digestive enzymes. Capsule endoscope is swallowed into the human digestive tract, so the simplified human tissue model needs to be established in the HFSS simulation software. In the figure 7 (b), a simplified three-tier organization model is established. The
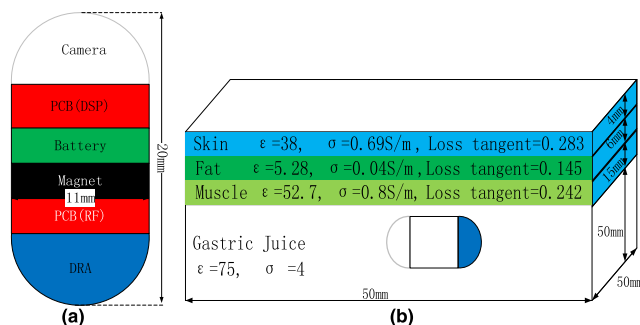

FIGURE 7. (a) WCE system structure diagram; (b) Structure diagram of three-layer organization simulation model.
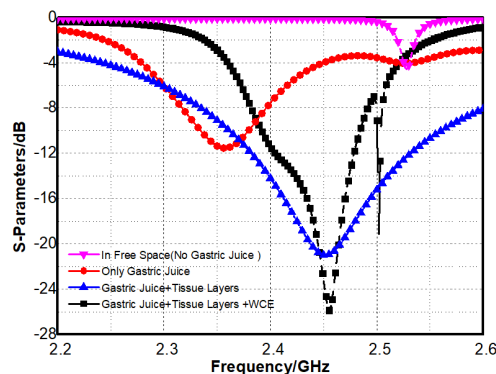

FIGURE 8. Reflection coefficient of the proposed antenna with different conditions.

capsule endoscope is placed in the stomach fluid. The size of the hexahedral model is 50 mm × 50 mm × 75mm, with skin of 4 mm, fat thickness of 6 mm and muscle thickness of 15 mm. Human tissue is the dispersion medium, so its electrical conductivity and relative permittivity change with the change of frequency. However, antenna working band (2.45 GHz ISM) is narrow, the electrical characteristics parameters of human tissue approximation is set at the center frequency of 2.45 GHz. Figure 7 (b) shows the specific relative dielectric constant and conductivity of the skin, fat and muscle, and gastric juice at the 2.45GHz.

The simulated results of S11 with different conditions are shown in Figure 8. The impedance matching varies with different conditions. The results of S11 in free space and gastric fluid are compared. Dielectric resonance antenna has higher external permittivity with gastric fluid, skin, muscle and other human tissues than in free space. So the resonant frequency of antenna in free space will shift towards high frequency. Effect of human tissue on reflection coefficients of antenna can be seen from the simulation results of S11 that in the case of three layers of tissue and gastric juice with the same size and only gastric juice. The resonance frequency is lower and the mismatching without than with the tissue layers, which is caused by the dielectric constant of the tissue layers. The performance of S11 does not vary much with or without the
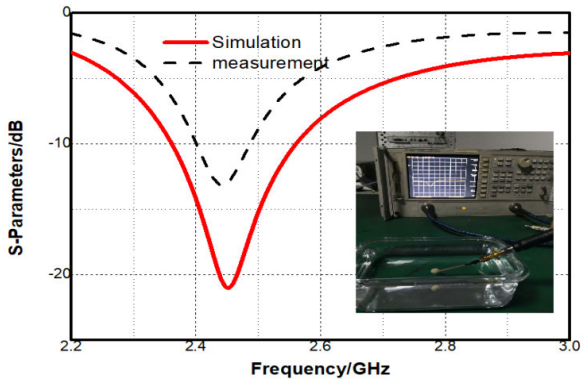
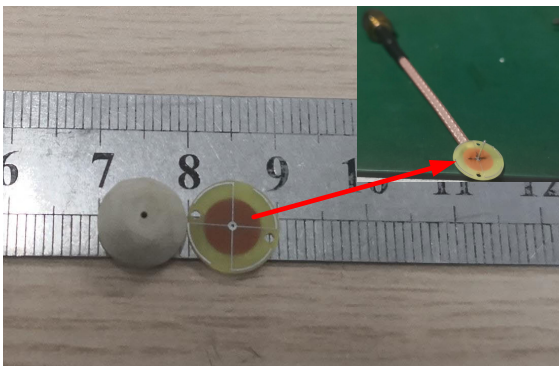**FIGURE 9.** Reflection coefficients of the proposed antenna.

FIGURE 10. (a) WCE system structure diagram; (b) Structure diagram of three-layer organization simulation model.
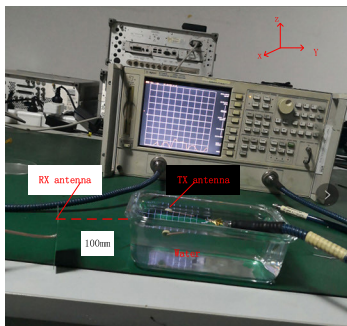

FIGURE 11. Transmission coefficient (S21) of the communication links when the capsule antenna is rotated in different orientations.

WCE system model, indicating that the proposed antenna is robust and suitable for the WCE system.

IV. RESULTS AND DISCUSSION

The simulated and measured reflection coefficients of the proposed and the external receiving antenna are shown in figure 9. The proposed antenna has the measured bandwidth (2.4–2.48 GHz). The measured reflection coefficients the resonance depth is worse than the simulation. The main cause of this problem is machining error. The actual machined dimensions and shape of the antenna are shown in Figure 10.

TABLE 2. The measurement of link loss S21 at 2.4GHz.

	0^0(dB)	45^0(dB)	90^0(dB)
xoy-plane	-33.2	-34.2	-42.4
yoz-plane	-35.1	-41.6	-38.7
xoz-plane	-34.5	-35.2	-36.8

FIGURE 12. The received power is compared when flexible monopole antenna and dielectric resonance antenna as transmitting antenna, respectively.

As shown in figure 11, the external antenna is set 100 mm far away from the capsule antenna. 100 mm is far enough to guarantee the distance between the capsule antenna in the human stomach tissue and the external antenna. The coordination system is also established in figure 11. To simplify the measurement, the communication links were only measured in some representative situations. The axis of the capsule is defined as the orientation of the antenna. During the measurement, the antenna is rotated in different orientations, while the external antenna orientation stays the same. Measured communication links in terms of S21 at the resonant frequency 2.4 GHz of various orientations and rotation angles are tabulated in Tables 2.

In order to further verify the performance of the antenna, the capsule endoscope system with different antennas is placed in water to measure. The signal radiated by the capsule endoscope is received by the receiving antenna and sent to the Spectrum Analyzer (FSH4), as shown in figure 12. When other conditions remain unchanged, the receiving power of the dielectric resonant antenna as the transmitting antenna is higher than the traditional flexible monopole.

Figure 13 is the measurement photograph and radiation pattern of passive antenna in microwave anechoic chamber when it is in water. Figure 13 (b) is a radiation pattern without normalization. The value represents the level value, not the gain. E-theta and E-phi represent the radiation pattern of horizontal polarization and vertical polarization, respectively. From this measurement radiation pattern, it can be concluded that the antenna radiate dual polarized electromagnetic wave. The radiation efficiency of the antenna is between 15-18%, and the peak gain is between −13.5 and −15dBi.

In order to show the advantage of the proposed antenna, Table 3 compares it with the capsule endoscope antennas in the published papers. The antenna in [4] has a wide BW, but it
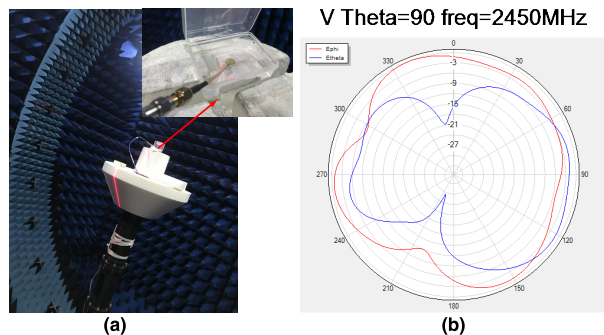
FIGURE 13. Measurement of radiation pattern. (a) Picture of measurement environment, (b) Radiation pattern at 2.45GHz.

TABLE 3. Performance comparison of the proposed DP antenna with capsule endoscope antennas.

Ref.	Size	Band width GHz	Polariz ation	Radiatio n	Type	Gain (dBi)
[4]	14.2mm× 16.6mm	2.08-2.86	CP	directio nal	Confo rmal	-29
[6]	11mm×2 2mm	0.7-1.7	linear	omnidir ectional	coppe r cylind e	-28
[8]	120 mm³	2.42-2.48	linear	omnidir ectional	PCB	N/A
[9]	225 mm²	433.05– 434.79	DP	omnidir ectional	Confo rmal	-38
[12]	128	2.36–2.44	DP	directio nal	Confo rmal	N/A
[13]	417 mm²	401–406, 902–928, 2.4–2.5	linear	omnidir ectional	Confo rmal	-30
Our s	157 mm³	2.4-2.5	DP	omnidir ectional	DRA	-15

has directional radiation pattern. Among the conformal antennas, the antenna in [9] radiation pattern distortion because of electronic components have serious effects on the radiation performance of the antenna.

V. CONCLUSION

In this paper, $TM_{01\delta}$ mode and $TE_{01\delta}$ mode have been used in DP omnidirectional DRA. The proposed antenna, together with parameters, electric field, SAR and the WCE system, has been analysed and discussed through HFSS simulation. The antenna is different from other types of the previous one (thin film, PCB, conformal antenna and so on). And it is simple structure and easy to manufacture, and not susceptible to external environment. The simulated results in three organs indicated that the proposed antenna is very stable and suitable for the WCE system. Finally, the fabricated antenna was measured in water. The polarization characteristic of the proposed antenna has been verified by measuring its communication links at different orientations. Variation of

communication links in terms of S21 is within 9dB. The measured results exhibit good properties of the WCE. The antenna gain, radiation pattern and efficiency measurement results are consistent with the simulation results. At the same time, the dielectric resonant antenna is compared with the flexible monopole antenna in combination with WCE. It is proved that the resonant antenna has higher gain than flexible monopole antenna.

REFERENCES

[1] G. R. Zuckerman, C. Prakash, M. P. Askin, and B. S. Lewis, "AGA technical review on the evaluation and management of occult and obscure gastrointestinal bleeding," *Gastroenterology*, vol. 118, no. 1, pp. 201–221, Jan. 2000.

[2] N. M. Munoz, "Capsule endoscopy," *World J. Gastroenterol.*, vol. 15, pp. 1584–1586, Apr. 2009.

[3] S. H. Lee, J. Lee, Y. J. Yoon, S. Park, C. Cheon, K. Kim, and S. Nam, "A wideband spiral antenna for ingestible capsule endoscope systems: Experimental results in a human phantom and a pig," *IEEE Trans. Biomed. Eng.*, vol. 58, no. 6, pp. 1734–1741, Jun. 2011.

[4] R. Li, Y.-X. Guo, and G. Du, "A conformal circularly polarized antenna for wireless capsule endoscope systems," *IEEE Trans. Antennas Propag.*, vol. 66, no. 4, pp. 2119–2124, Apr. 2018.

[5] M. Basar, M. Ahmad, J. Cho, and F. Ibrahim, "Application of wireless power transmission systems in wireless capsule endoscopy: An overview," *Sensors*, vol. 14, no. 6, pp. 10929–10951, Jun. 2014.

[6] Z. Duan, L.-J. Xu, S. Gao, and W. Geyi, "Integrated design of wideband omnidirectional antenna and electronic components for wireless capsule endoscopy systems," *IEEE Access*, vol. 6, pp. 29626–29636, 2018.

[7] R. Li, Y.-X. Guo, B. Zhang, and G. Du, "A miniaturized circularly polarized implantable annular-ring antenna," *IEEE Antennas Wireless Propag. Lett.*, vol. 16, pp. 2566–2569, 2017.

[8] W. Cui, R. Liu, L. Wang, M. Wang, H. Zheng, and E. Li, "Design of wideband implantable antenna for wireless capsule endoscope system," *IEEE Antennas Wireless Propag. Lett.*, vol. 18, no. 12, pp. 2706–2710, Dec. 2019.

[9] W. Lei and Y.-X. Guo, "Design of a dual-polarized wideband conformal loop antenna for capsule endoscopy systems," *IEEE Trans. Antennas Propag.*, vol. 66, no. 11, pp. 5706–5715, Nov. 2018.

[10] G. Iddan, G. Meron, P. Swain, and A. Glukhovsky, "Wireless capsule endoscopy," *Nature*, vol. 405, no. 6785, p. 417, 2000.

[11] C. Liu, Y.-X. Guo, R. Jegadeesan, and S. Xiao, "*In vivo* testing of circularly polarized implantable antennas in rats," *IEEE Antennas Wireless Propag. Lett.*, vol. 14, pp. 783–786, 2015.

[12] Y. Li, Y.-X. Guo, and S. Xiao, "Orientation insensitive antenna with polarization diversity for wireless capsule endoscope system," *IEEE Trans. Antennas Propag.*, vol. 65, no. 7, pp. 3738–3743, Jul. 2017.

[13] Z. Bao, Y.-X. Guo, and R. Mittra, "Single-layer dual-/tri-band inverted-F antennas for conformal capsule type of applications," *IEEE Trans. Antennas Propag.*, vol. 65, no. 12, pp. 7257–7265, Dec. 2017.

[14] L.-J. Xu, Y.-X. Guo, and W. Wu, "Bandwidth enhancement of an implantable antenna," *IEEE Antennas Wireless Propag. Lett.*, vol. 14, pp. 1510–1513, 2015.

[15] Y. H. Jung, Y. Qiu, S. Lee, T.-Y. Shih, Y. Xu, R. Xu, J. Lee, A. A. Schendel, W. Lin, J. C. Williams, N. Behdad, and Z. Ma, "A compact parylene-coated WLAN flexible antenna for implantable electronics," *IEEE Antennas Wireless Propag. Lett.*, vol. 15, pp. 1382–1385, 2016.

[16] H. Li, Y.-X. Guo, C. Liu, S. Xiao, and L. Li, "A miniature-implantable antenna for MedRadio-band biomedical telemetry," *IEEE Antennas Wireless Propag. Lett.*, vol. 14, pp. 1176–1179, 2015.

[17] K. Zhang, C. Liu, X. Liu, H. Cao, Y. Zhang, X. Yang, and H. Guo, "A conformal differentially fed antenna for ingestible capsule system," *IEEE Trans. Antennas Propag.*, vol. 66, no. 4, pp. 1695–1703, Apr. 2018.

[18] J. Shang and Y. Yu, "An ultrawideband capsule antenna for biomedical applications," *IEEE Antennas Wireless Propag. Lett.*, vol. 18, no. 12, pp. 2548–2551, Dec. 2019.

[19] W. Li, K. W. Leung, and N. Yang, "Omnidirectional dielectric resonator antenna with a planar feed for circular polarization diversity design," *IEEE Trans. Antennas Propag.*, vol. 66, no. 3, pp. 1189–1197, Mar. 2018.

[20] T. Liu, H. Yang, Y. He, and J. Lu, "A $TE_{01\delta}$ mode omnidirectional dielectric resonator antenna excited by a special configuration," *IEEE Trans. Antennas Propag.*, vol. 66, no. 12, pp. 7339–7341, Dec. 2018.

[21] G. Varshney, V. S. Pandey, R. S. Yaduvanshi, and L. Kumar, "Wide band circularly polarized dielectric resonator antenna with stair-shaped slot excitation," *IEEE Trans. Antennas Propag.*, vol. 65, no. 3, pp. 1380–1383, Mar. 2017.

[22] I. Ali, M. H. Jamaluddin, A. Gaya, and H. A. Rahim, "A dielectric resonator antenna with enhanced gain and bandwidth for 5G applications," *Sensors*, vol. 20, no. 3, p. 675, Jan. 2020.

[23] A. Iqbal, A. Smida, O. Saraereh, Q. Alsafasfeh, N. Mallat, and B. Lee, "Cylindrical dielectric resonator antenna-based sensors for liquid chemical detection," *Sensors*, vol. 19, no. 5, p. 1200, Mar. 2019.

[24] A. Altaf and M. Seo, "Dual-band circularly polarized dielectric resonator antenna for WLAN and WiMAX applications," *Sensors*, vol. 20, no. 4, p. 1137, Feb. 2020.

[25] A. Altaf, J.-W. Jung, Y. Yang, K.-Y. Lee, and K. Hwang, "Vertical-strip-fed broadband circularly polarized dielectric resonator antenna," *Sensors*, vol. 17, no. 8, p. 1911, Aug. 2017.

[26] *IEEE Standard for Safety Levels With Respect to Human Exposure to Radio Frequency Electromagnetic Fields, 3 kHz to 300 GHz*, IEEE Standard C95.1-2005 (Revision of IEEE Std C95.1-1991), Apr. 2006, pp. 1–238, doi: 10.1109/IEEESTD.2006.99501.

KEJIA ZHAO was born in Shaoxing, Zhejiang, China, in 1992. She received the Master of Internal Medicine from the Zhejiang Chinese Medical University, China, in 2019. She has been a Gastroenterologist with the Zhejiang Hospital, China. Her research interests include pathophysiological manifestations and clinical mechanisms of gastrointestinal diseases.

HAO JIANG was born in Zhoushan, Zhejiang, China, in 1980. He received the B.S. degree in clinical medicine from the Zhejiang University of Traditional Chinese Medicine, China, in 2004, and the M.S. and Ph.D. degrees in oncology from the Zhejiang University of Traditional Chinese Medicine, in 2008 and 2011, respectively. From 2011 to 2015, he was an Attending Physician of oncology with the Department of Oncology, Zhejiang Hospital, Zhejiang, China, where he has been an Associate Chief Physician of oncology, since 2015. He is the author of more than 50 articles. His research interest includes electromagnetic field physiotherapy for tumors.

LITING CHEN was born in Jiaxin, Zhejiang, China, in 1990. She received the master's degree in clinical medicine from Zhejiang University, in 2015. Since 2015, she has been an oncologist with the Department of Oncology, Zhejiang Hospital, China. She is the author of two articles. Her research interest includes hyperthermia development of cancer treatment.

JIANJUN LAI was born in Anlu, Hubei, China, in 1984. He received the B.S. degree in medical imaging from the University of Wenzhou Medical, China, in 2011, and the M.S. degree in electronic and communications engineering from the Zhejiang University of Technology, China, in 2016. From 2012 to 2017, he was an Assistant Engineer of medical physics with the Department of Radiation Oncology, Hangzhou Cancer Hospital, Zhejiang, China. Since 2017, he has been an Engineer of medical physics with the Department of Radiation Oncology, Zhejiang Hospital, China. He is the author of more than 40 articles and more than ten inventions. His research interests include biomedical instrument development and biomedical image processing.

ZHIBING WU was born in Huzhou, Zhejiang, China, in 1977. He received the B.S. degree in clinical medicine from Zhejiang University, China, in 2003, and the M.S. and Ph.D. degrees in oncology from the Zhejiang University of Traditional Chinese Medicine, China, in 2010. From 2006 to 2011, he was an Attending Physician of oncology with the Department of Radiation Oncology, Zhejiang Cancer Hospital, Zhejiang, China. Since 2019, he has been the Chief Physician of oncology with the Department of Oncology, Zhejiang Hospital, China. He is the author of more than 70 articles and more than ten inventions. His research interest includes electromagnetic field physiotherapy for tumors.

JI WANG was born in Hangzhou, Zhejiang, China, in 1977. He received the B.S. degree in computer science and technology from China Central Radio and Television University, China, in 2007, and the M.S. degree in electronic and communications engineering from the Shanghai University of Science and Technology, China, in 2015. From 2005 to 2012, he was an Engineer of equipment research and development with the Equipment Department, Hangzhou Red Cross Society Hospital, Zhejiang, China. Since 2015, he has been a Senior Engineer of medical equipment research and development with the Department of Medical Engineering, Zhejiang Hospital, China. He is the author of more than 30 articles and more than three inventions. His research interest includes medical device research and development.

JIPING LIU was born in Hangzhou, Zhejiang, China, in 1982. He received the bachelor's degree in medicine from Wenzhou Medical University, in 2008. He currently works as a Senior Engineer of medical physics (an Associate Senior Technologist) with the Medical Physicist Department, Zhejiang Cancer Hospital. He is the author of more than 15 articles and two inventions. His research interests include physic therapeutics and techniques of radiotherapy for cancer. From 2013 to 2015, he was the 23-rd Team of China Medical aid to Mali, with the Chief Engineer of Radiotherapy Department. In May 2017, he was the Vice Director of the Medical Physicist Department, Zhejiang Cancer Hospital. In 2019, he was with the FOX Chase Cancer Centre of American, as a Visiting Scholar.

● ● ●